Am J Cancer Res 2025;15(4):1902-1918
www.ajcr.us /ISSN:2156-6976/ajcr0163494

Original Article

Autophagy-dependent apoptosis induction by oridonin are mediated by ROS-dependent AMPK-mTOR-ULK1 pathway in colon cancer

Bin Shao, Heqi Bu, Ganglei Li, Dapeng Kang, Qi Ju

Department of Colorectal Surgery, Beilun District People's Hospital (Beilun Branch of The First Affiliated Hospital of Zhejiang University School of Medicine), Ningbo 315800, Zhejiang, The People's Republic of China

Received January 22, 2025; Accepted April 17, 2025; Epub April 25, 2025; Published April 30, 2025

Abstract: Oridonin, a bioactive diterpenoid isolated from Rabdosia species, exhibits broad-spectrum anticancer activity across various tumor types. However, its impact on colon cancer and the underlying molecular mechanisms remains poorly understood. Our study revealed that oridonin significantly suppressed the proliferation of HCT8 and HCT116 colon cancer cells by inducing G2/M phase cell cycle arrest. Moreover, oridonin triggered apoptotic cell death, as indicated by elevated levels of cleaved caspase-3 and PARP. Simultaneously, it activated autophagy, as evidenced by increased expression of Beclin 1 and LC3-II, along with decreased LC3-I and p62 levels. In addition, inhibiting autophagy with 3-methyladenine (3-MA) reduced cell apoptosis, whereas blocking apoptosis using Z-Val-Ala-Asp(OMe)-FMK (Z-VAD-FMK) enhanced autophagy. Furthermore, oridonin also induced the accumulation of reactive oxygen species (ROS), which contributed to apoptosis; this effect was largely reversed by the ROS scavenger N-acetyl-L-cysteine (NAC). Mechanistically, oridonin increased phosphorylation of AMP-activated protein kinase (AMPK) and suppressed phosphorylation of mammalian target of rapamycin (mTOR) and Unc-51-like kinase 1 (ULK1). Silencing AMPK with siRNA blocked oridonin's effects on the AMPK/mTOR pathway, as well as its regulation of autophagy and apoptosis. Moreover, co-treatment with NAC almost completely blocked activation of the AMPK-mTOR-ULK1 signaling pathway. In vivo, oridonin significantly suppressed tumor growth in a xenograft model, accompanied by elevated expression of LC3-II and cleaved caspase-3. Collectively, these findings demonstrated that oridonin could exert potent anti-tumor effects in colon cancer by inducing cell cycle arrest and promoting autophagy-dependent apoptosis via ROS-mediated activation of the AMPK-mTOR-ULK1 signaling pathway.

Keywords: Oridonin, Colon cancer, apoptosis, autophagy, reactive oxygen species (ROS)

Introduction

Colorectal cancer is a leading cause of cancer-related mortality worldwide, with incidence rates continuing to rise [1]. Despite recent advances in early detection and therapeutic strategies, treatment outcomes for patients with advanced colorectal cancer remain unsatisfactory, largely due to severe toxicity, multidrug resistance, and high rates of recurrence and metastasis. Therefore, uncovering the mechanisms underlying tumor proliferation and identifying effective anticancer agents remain critical research priorities with significant clinical implications [2].

Autophagy and apoptosis are two key forms of programmed cell death closely linked to cancer cell survival, growth, differentiation, and proliferation [3]. These pathways can be activated independently or simultaneously in response to various cellular stresses [4]. Autophagy plays a complex role in tumor biology, acting either as a cytoprotective mechanism that supports cancer cell survival or as a cytotoxic process that promotes cancer cell death [5]. The interplay between apoptosis and autophagy may ultimately determine the fate of cancer cells, although the precise mechanisms governing this crosstalk require further investigation.

Reactive oxygen species (ROS) function as critical signaling molecules that regulate numerous intracellular pathways [6]. Elevated ROS levels influence both autophagy and apoptosis, playing a pivotal role in tumor initiation and progres-

https://doi.org/10.62347/CGIO2604

sion [7, 8]. AMP-activated protein kinase (AMPK), a key energy sensor, maintains ATP homeostasis and coordinates metabolic stress responses. In cancer, AMPK exhibits dual roles in tumor development and therapeutic resistance, making it a promising target for anticancer interventions [9]. Mammalian target of rapamycin (mTOR), a central regulator of cell growth and metabolism, is frequently used by tumor cells to sustain proliferation [10]. Excessive ROS can activate AMPK and related pathways, inducing autophagy and apoptosis to suppress tumor growth [11]. For example, artesunate has been shown to promote autophagy-dependent cell death in human bladder carcinoma by elevating ROS and activating AMPK/mTOR/Unc-51-like kinase 1 (ULK1) signaling [12], while hernandezine induces autophagic death in pancreatic cancer cells via ROS-dependent AMPK activation [13]. Recent evidence indicates that traditional Chinese medicines can induce both apoptotic and autophagic death in colorectal cancer through modulation of the ROS-AMPK-mTOR axis [14, 15].

Natural products, known for their high efficacy and low toxicity, are widely explored as anticancer agents [2]. Oridonin, a bioactive diterpenoid isolated from *Rabdosia* species, exhibits anti-inflammatory, antibacterial, and potent anticancer properties, and has been widely investigated across various malignancies [16]. Its anti-proliferative and pro-apoptotic effects in colon cancer have been demonstrated both *in vitro* and *in vivo* [17-19]. Our recent studies have confirmed that oridonin triggers apoptosis through autophagy-dependent mechanisms in DLD-1 colon cancer cells by activating the AMPK-mTOR-ULK1 axis [20]. However, whether ROS accumulation contributes to this mechanism remains unclear. In the present study, we aimed to determine the role of ROS as a critical mediator of oridonin-induced effects in colon cancer, including apoptosis, autophagy activation, and cell cycle arrest. These findings may offer new insights into the development of targeted therapies for colon cancer.

Materials and methods

Reagents and antibodies

Oridonin (purity >98%, P0290) was purchased from Shanghai PureOne Biotechnology Co., Ltd. and dissolved in 0.5% dimethyl sulfoxide (DMSO) to prepare a 10 mM stock solution. Dulbecco's Modified Eagle Medium (DMEM) supplemented with penicillin/streptomycin, 10% fetal bovine serum (FBS), 0.25% trypsin, and DMSO were obtained from Abcam (UK). The Cell Counting Kit-8 (CCK-8), Annexin V-FITC/propidium iodide (PI) apoptosis detection kit, ROS assay kit, bicinchoninic acid (BCA) protein assay kit, fluorescent dye monodansylcadaverine (MDC), N-acetyl-L-cysteine (NAC), 3-methyladenine (3-MA), Z-Val-Ala-Asp(OMe)-FMK (Z-VAD-FMK), and radioimmunoprecipitation assay (RIPA) lysis buffer were all purchased from Sigma-Aldrich (USA). The enhanced chemiluminescence (ECL) detection kit was acquired from PerkinElmer (USA). Rabbit monoclonal antibodies against GAPDH (Cat. No. 2118), cleaved caspase-3 (Cat. No. 94530), cleaved PARP (Cat. No. 9664), LC3B (Cat. No. 2775), Beclin1 (Cat. No. 3738), p62 (Cat. No. 5114), phosphorylated mTOR (p-mTOR, Cat. No. 3056), mTOR (Cat. No. 2971), phosphorylated AMPK (p-AMPK, Cat. No. 2835), AMPK (Cat. No. 2532), phosphorylated ULK1 (p-ULK1, Cat. No. 6888), ULK1 (Cat. No. 8054), and horseradish peroxidase (HRP)-conjugated goat anti-rabbit IgG (Cat. No. 5064) were obtained from Cell Signaling Technology (USA).

Cell culture

Human colon cancer cell lines HCT116 and HCT8, as well as the normal human colon epithelial cell line CRL-1790, were obtained from the American Type Culture Collection (ATCC). Cells were cultured in DMEM supplemented with 10% FBS, 100 μg/mL streptomycin, and 100 IU/mL penicillin at 37°C in a humidified atmosphere containing 5% CO_2. The medium was replaced every 2-3 days. Cells were subcultured using 0.25% trypsin when confluence reached approximately 80%.

CCK-8 assay

HCT116, HCT8, and CRL-1790 cells were seeded into 96-well plates at 5×10^3 cells/well and incubated overnight. Cells were treated with various concentrations of oridonin (0, 5, 10, 15, 20, and 25 μM) for 24, 48, or 72 hours. At each time point, 10 μL of CCK-8 solution was added to each well, followed by a 4-hour incubation. The absorbance at 450 nm was measured using a microplate reader.

Colony formation assay

HCT116 and HCT8 cells (1×10^3 cells/well) were seeded into 6-well plates and incubated overnight. Cells were then treated with oridonin (0, 10, 15, or 20 μM) for two weeks. Colonies were washed with phosphate-buffered saline (PBS), fixed with methanol for 20 minutes, and stained with 0.5% crystal violet. Colonies were imaged and counted under a microscope.

EdU incorporation assay

HCT116 and HCT8 cells (1×10^4 cells/well) were seeded into 96-well plates and treated with oridonin for 48 hours. Cells were incubated with 10 μM EdU for 2 hours, then fixed, incubated with 2 mg/mL glycine, and washed with PBS. Cells were stained with Apollo reaction solution, followed by DAPI staining (1 mg/mL) for 30 minutes in the dark. EdU-positive cells were visualized using fluorescence microscopy.

Cell cycle analysis

HCT116 and HCT8 cells (5×10^5 cells/well) were seeded into 6-well plates and treated with oridonin (0, 10, 15, or 20 μM) for 24 hours. Cells were harvested, fixed overnight in 70% ethanol at 4°C, washed, and stained with PI/RNase solution for 30 minutes in the dark. DNA content was analyzed by flow cytometry (BD, USA).

Cell apoptosis analysis

HCT116 and HCT8 cells (5×10^5 cells/well) were treated with oridonin (0, 10, 15, or 20 μM) with or without 2 mM 3-MA for 48 hours. Cells were collected, resuspended in binding buffer (1×10^5 cells), and stained with 5 μL Annexin V-FITC and 10 μL PI for 30 minutes in the dark at room temperature. Apoptosis was analyzed using flow cytometry.

MDC staining

HCT116 and HCT8 cells (1×10^4 cells/well) were seeded in 6-well plates and treated with oridonin (0 or 20 μM), alone or in combination with 2 mM 3-MA or 20 μM Z-VAD-FMK for 48 hours. Cells were incubated with 50 μM MDC dye in fresh medium for 30 minutes at room temperature in the dark, washed with PBS, and examined under a confocal microscope.

Measurement of ROS

ROS levels were measured using a ROS assay kit. HCT116 and HCT8 cells were seeded into 6-well plates and treated with oridonin (with or without 5 mM NAC) for 48 hours. After incubation with 10 μM DCFH-DA probe at 37°C for 30 minutes in the dark, cells were washed with PBS, and fluorescence was measured using a flow cytometer (excitation: 488 nm; emission: 535 nm).

RNA interference

HCT116 and HCT8 cells (~2×10^5/well) were transfected with AMPK-specific or scrambled small interfering RNA (siRNA) oligonucleotides (20 nM) using Lipofectamine 2000 according to the manufacturer's instructions. After 6-8 hours, the medium was replaced with fresh medium containing 20 μM oridonin. Cells were incubated for 48 hours before analysis.

Western blotting analysis

Cells or xenograft tumor tissues were lysed in ice-cold RIPA buffer for 30 minutes and centrifuged at 12,000 rpm at 4°C for 5 minutes. Protein concentration was determined by BCA assay. Equal amounts of protein (40 μg) were separated by 12% sodium dodecyl sulfate-polyacrylamide gel electrophoresis (SDS-PAGE) and then transferred to polyvinylidene difluoride (PVDF) membranes. Membranes were blocked with 5% non-fat milk in TBST for 2 hours and incubated with primary antibodies (1:1000) at 4°C overnight, followed by HRP-conjugated secondary antibodies (1:5000) for 2 hours. Protein bands were visualized using ECL detection kit and quantified with ImageJ software.

Xenograft mouse model

Eighteen male BALB/c nude mice (5-6 weeks old, 18-20 g) were procured from Shanghai Slack Experimental Animals Center and housed under specific pathogen-free (SPF) conditions (temperature: 21-25°C; humidity: 60-65%; 12 h light/dark cycle) with free access to food and water. After one week of acclimatization, HCT8 cells (2×10^6) were subcutaneously injected into the right flank of each mouse. When tumors reached ~100 mm^3, mice were randomly divided into three groups (n = 6 per group) and treat-

ed intraperitoneally with oridonin (5 or 10 mg/kg) or saline (control) for 3 weeks. Tumor size was measured weekly using calipers, and volume was calculated as $V = ½ \times \text{length} \times \text{width}^2$. At the end of the experiment, mice were euthanized by cervical dislocation, and their tumors were excised, photographed, weighed, and snap-frozen in liquid nitrogen for protein analysis.

Statistical analysis

Data were presented as mean ± standard deviation (SD). Statistical analyses were performed using SPSS 18.0 and ImageJ software. Comparisons between two groups were made using the unpaired Student's t-test, while one-way analysis of variance (ANOVA) was used for multiple-group comparisons. A *p*-value of <0.05 was considered statistically significant.

Results

Oridonin inhibited proliferation in colon cancer cells

Cell viability was assessed using the CCK-8 assay after treatment with varying concentrations of oridonin in HCT116, HCT8, and CRL-1790 cells for 24, 48, and 72 hours, respectively. As shown in **Figure 1A**, oridonin exerted dose- and time-dependent antiproliferative effects on both HCT8 and HCT116 cell lines, with 48-hour half-maximal inhibitory concentration (IC_{50}) values of 18.64±2.26 μM and 23.75±3.07 μM, respectively. In contrast, oridonin showed no significant cytotoxic effects on normal human colon epithelial cells (CRL-1790). Based on these findings, concentrations of 10-20 μM were selected for subsequent experiments. Colony formation assays demonstrated a concentration-dependent reduction in colony-forming ability in HCT116 and HCT8 cells following oridonin treatment (**Figure 1B**). Similarly, EdU incorporation assays revealed a significant decrease in the proportion of EdU-positive cells in both cell lines (**Figure 1C**).

Oridonin induced G2/M phase cell cycle arrest in colon cancer cells

Flow cytometry analysis was performed to evaluate cell cycle distribution in HCT116 and HCT8 cells treated with increasing concentrations of oridonin (0, 10, 15, and 20 μM) for 24 hours. The proportion of cells in the G2/M phase increased significantly in both cell lines following oridonin treatment, indicating that oridonin induces cell cycle arrest at the G_2/M phase (**Figure 2**).

Oridonin triggered apoptosis and autophagy in colon cancer cells

Following 48 hours of treatment with oridonin (0-20 μM) and/or 3-MA (2 mM), apoptosis was evaluated in HCT8 and HCT116 cells using flow cytometry and Annexin V-FITC/PI staining. As shown in **Figure 3A** and **3B**, oridonin induced apoptosis in a dose-dependent manner, which was significantly reversed by co-treatment with 3-MA.

MDC, an eosinophilic dye that selectively binds to autophagic vesicles and stains acidic vacuoles, was used to evaluate autophagy formation. Under confocal microscopy, MDC fluorescence appears as punctate staining around the nucleus, allowing assessment of autophagic activity based on fluorescence intensity. After 48 hours of oridonin treatment, MDC staining revealed a significant increase in fluorescence intensity in both cell lines, indicating enhanced autophagic activity (**Figure 3E**).

Western blot analysis further demonstrated that oridonin treatment upregulated the expression levels of autophagy-related proteins Beclin-1 and LC3-II in a dose-dependent manner, while downregulating LC3-I and p62. Pro-apoptotic markers including cleaved caspase-3 and poly (ADP-ribose) polymerase (PARP) were significantly elevated. These effects were completely reversed by co-treatment with 3-MA (**Figure 3H**).

Oridonin induced autophagy-dependent apoptosis in colon cancer cells

HCT116 and HCT8 cells were treated with oridonin (0, 20 μM) with or without 3-MA (2 mM) or the pan-caspase inhibitor Z-VAD-FMK (20 μM) for 48 hours. The CCK-8 assay showed that 3-MA significantly reversed the anti-proliferative effects of oridonin (**Figure 3C** and **3D**). MDC fluorescence staining revealed that 3-MA significantly reduced the oridonin-induced accumulation of autophagosomes (**Figure 3F**) but had no effect on cell viability or autophagy. In contrast, co-treatment with Z-VAD-FMK

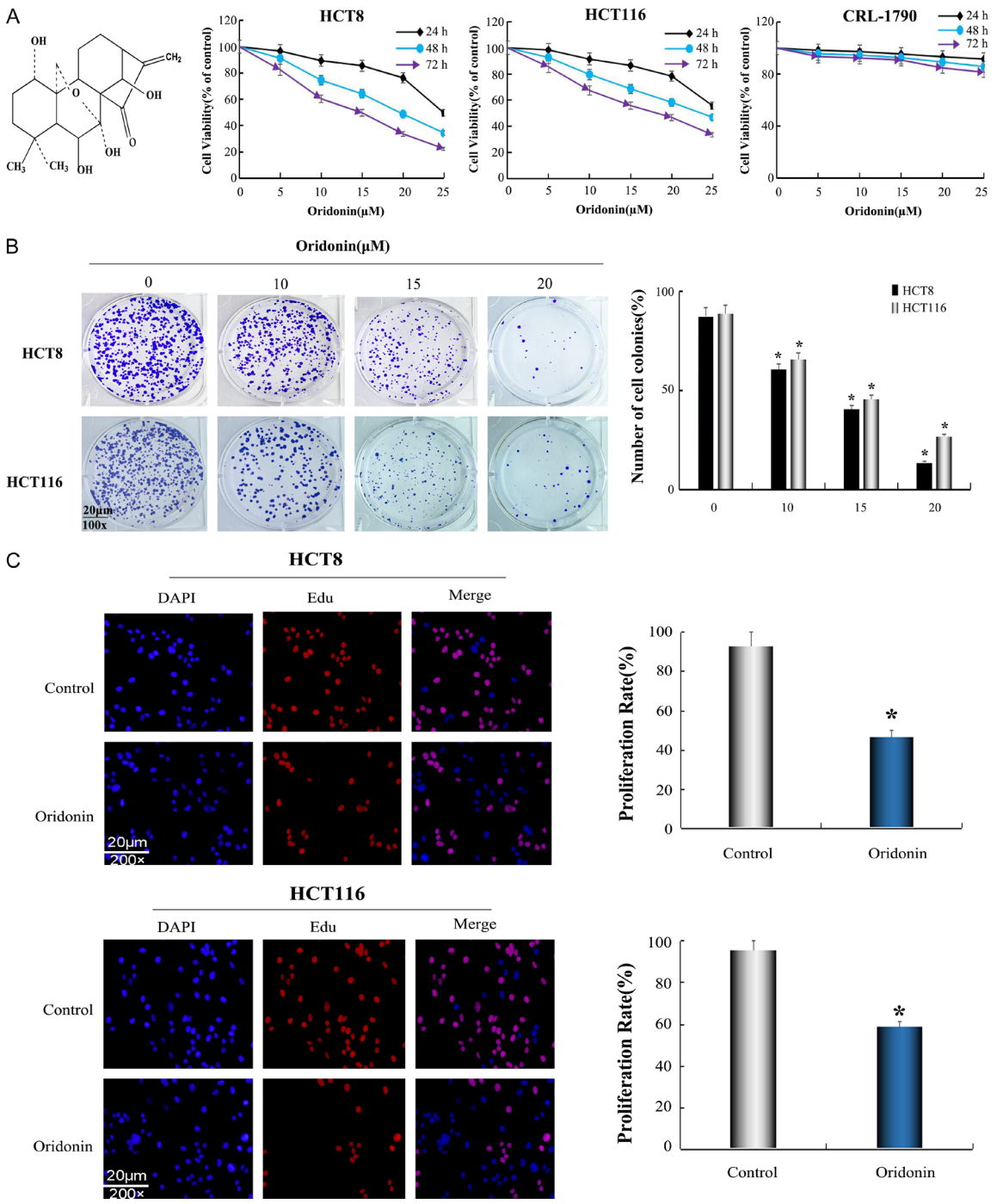

Figure 1. Oridonin inhibited proliferation in colon cancer. A. The chemical structure of oridonin. HCT116, HCT8 and CRL-1790 cells were exposed to various concentrations of oridonin (0, 5, 10, 15, 20 and 25 μM) for 24, 48 h and 72 h, respectively, and the cell viability of cells was assessed by CCK-8 assay. B. The colony formation was counted in HCT116 and HCT8 cells treated with oridonin. C. After 48 h of exposure to oridinin, and cell proliferation was further evaluated by EdU incorporation assay *P<0.05 vs control group.

increased oridonin-induced autophagosome accumulation (**Figure 3G**). Western blot analysis revealed that Z-VAD-FMK attenuated oridonin-induced cleavage of caspase-3 and PARP, while further increasing LC3-II expression (**Figure 3I**).

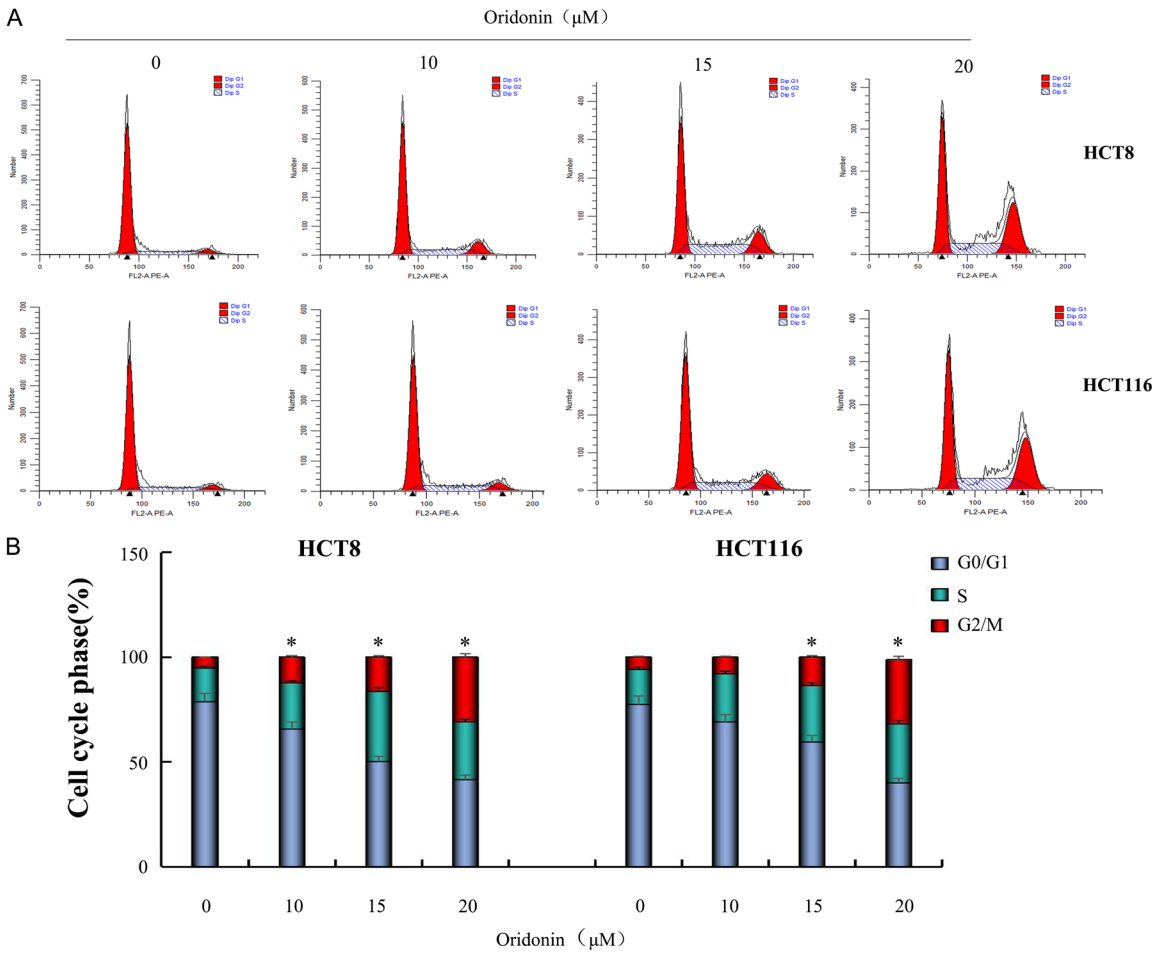

Figure 2. Oridonin caused G_2/M arrest in colon cancer. HCT116 and HCT8 cells were exposed to various concentrations of oridonin (0, 10, 15 and 20 μmol/L) for 24 h, and cell cycle was analyzed by flow cytometry. *P<0.05 vs control group.

ROS were involved in oridonin-induced apoptosis in colon cancer cells

After 48-hour treatment with oridonin (0, 10, 15, 20 μM) with or without the ROS scavenger NAC, flow cytometry analysis revealed a dose-dependent increase in intracellular ROS levels in both HCT8 and HCT116 cells, which was effectively suppressed by NAC (**Figure 4A**). In addition, oridonin-induced apoptosis was partially inhibited by NAC co-treatment (**Figure 4B**).

Oridonin inhibited cell proliferation via ROS-dependent activation of AMPK-mTOR-ULK1 axis

Western blot analysis demonstrated that 48-hour treatment with oridonin upregulated p-AMPK and downregulated p-mTOR and p-ULK1 in HCT8 and HCT116 cells (**Figure 5A**). Silencing AMPK reversed these changes, significantly decreasing p-AMPK, LC3-II, and apoptotic markers (cleaved caspase-3/PARP), while increasing p-mTOR, p-ULK1, and LC3-I expression compared to oridonin treatment alone (**Figure 5B**). CCK-8 results confirmed that AMPK knockdown partially restored cell viability compared to oridonin treatment alone (**Figure 5D**). Flow cytometry also showed a decrease in apoptosis upon AMPK silencing (**Figure 5C**). Furthermore, NAC co-treatment reduced p-AMPK expression and increased p-mTOR and p-ULK1 levels compared to oridonin treatment alone (**Figure 6**).

Oridonin suppressed xenograft tumor growth in vivo

To evaluate the *in vivo* anti-tumor effects of oridonin, a mouse xenograft model was estab-

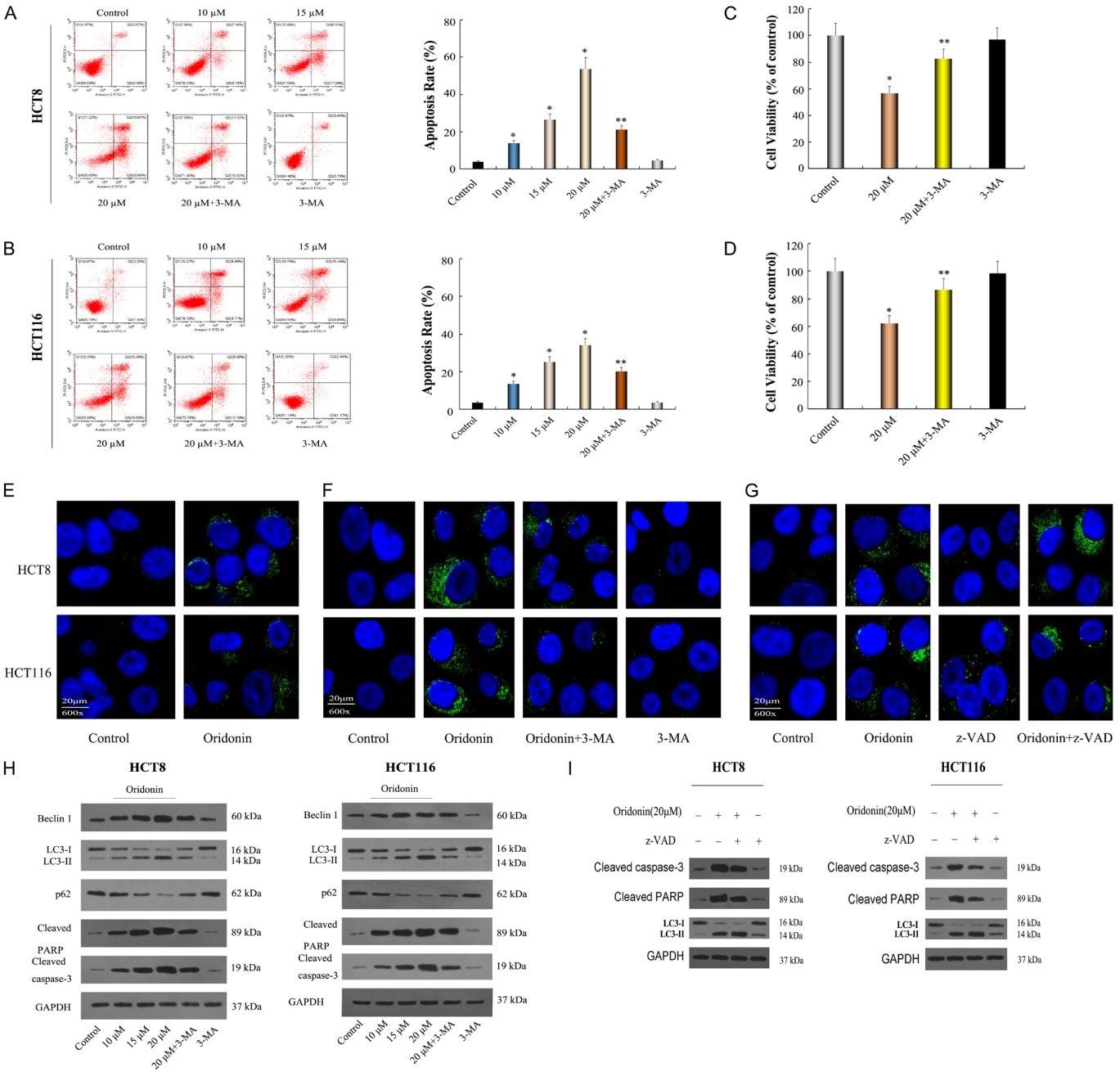
A
Control
10 μM
15 μM
HCT8
20 μM
20 μM+3-MA
3-MA
Apoptosis Rate (%)
Control
10 μM
15 μM
20 μM
20 μM+3-MA
3-MA
C
Cell Viability (% of control)
Control
20 μM
20 μM+3-MA
3-MA
B
HCT116
D
E
HCT8
HCT116
20μm
600x
Control
Oridonin
F
Oridonin+3-MA
3-MA
G
z-VAD
Oridonin+z-VAD
H
HCT8
HCT116
Oridonin
Beclin 1
60 kDa
LC3-I
LC3-II
16 kDa
14 kDa
p62
62 kDa
Cleaved
PARP
Cleaved
caspase-3
89 kDa
19 kDa
GAPDH
37 kDa
I
Oridonin(20μM)
z-VAD
Cleaved caspase-3
Cleaved PARP
LC3-I
LC3-II
GAPDH

Figure 3. Oridonin triggered autophagy-dependent apoptosis in colon cancer. HCT116 and HCT8 cells were exposed to various concentrations of oridonin (0, 10, 15 and 20 μM) or/and 2 mM 3-MA, 20 μM Z-VAD-FAMK for 48 h. A and B. Cell apoptosis was detected by flow cytometry with Annexin V-FITC/PI staining. C and D. Cell viability of cells was assessed by CCK-8 assay. E-G. Cell autophagy was evaluated by MDC staining. H and I. The expression levels of apoptosis- and autophagy-related proteins were measured by western blot analysis. *P<0.05 vs control group, **P<0.05 vs oridonin (20 μM) group.

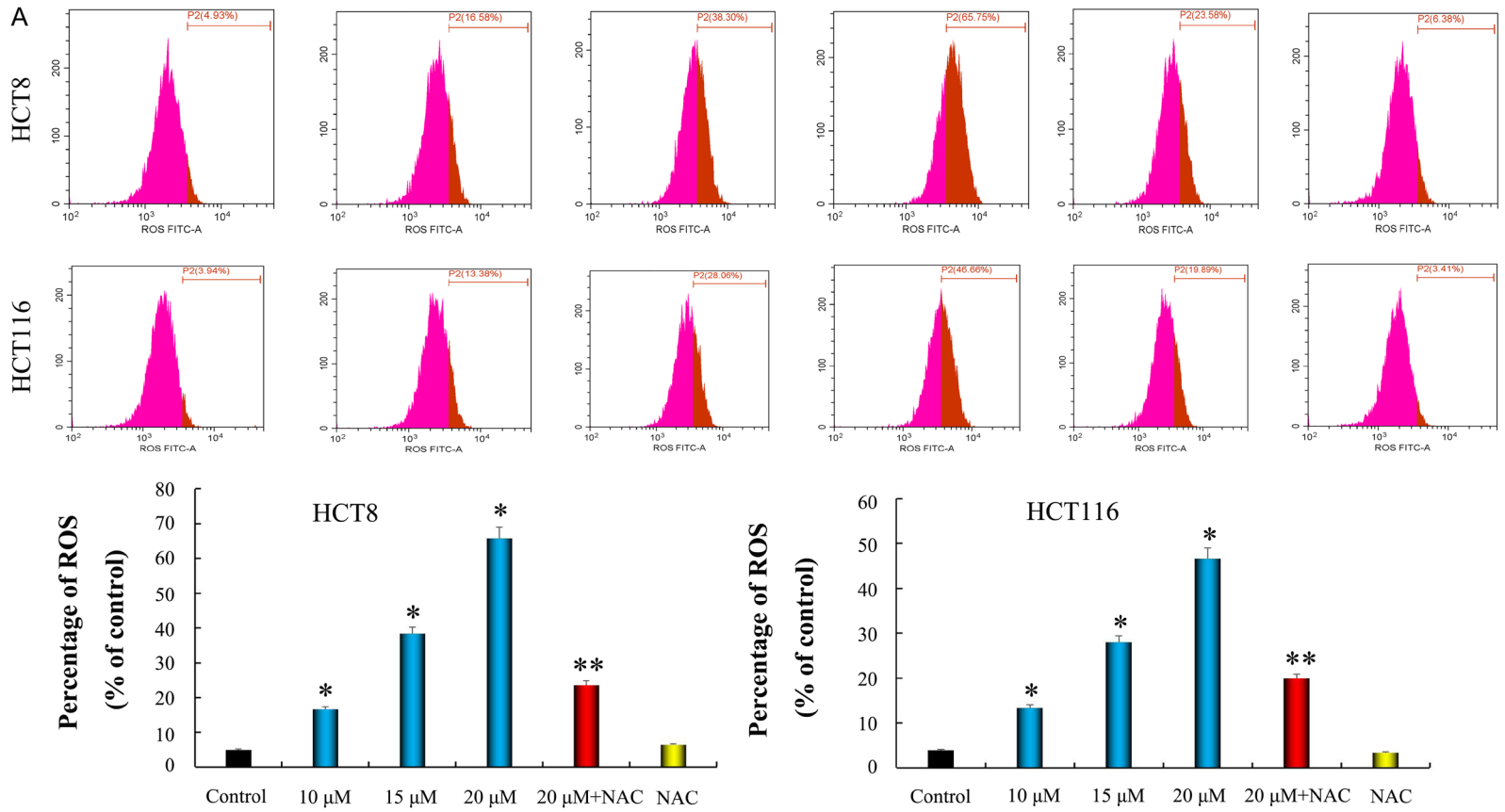

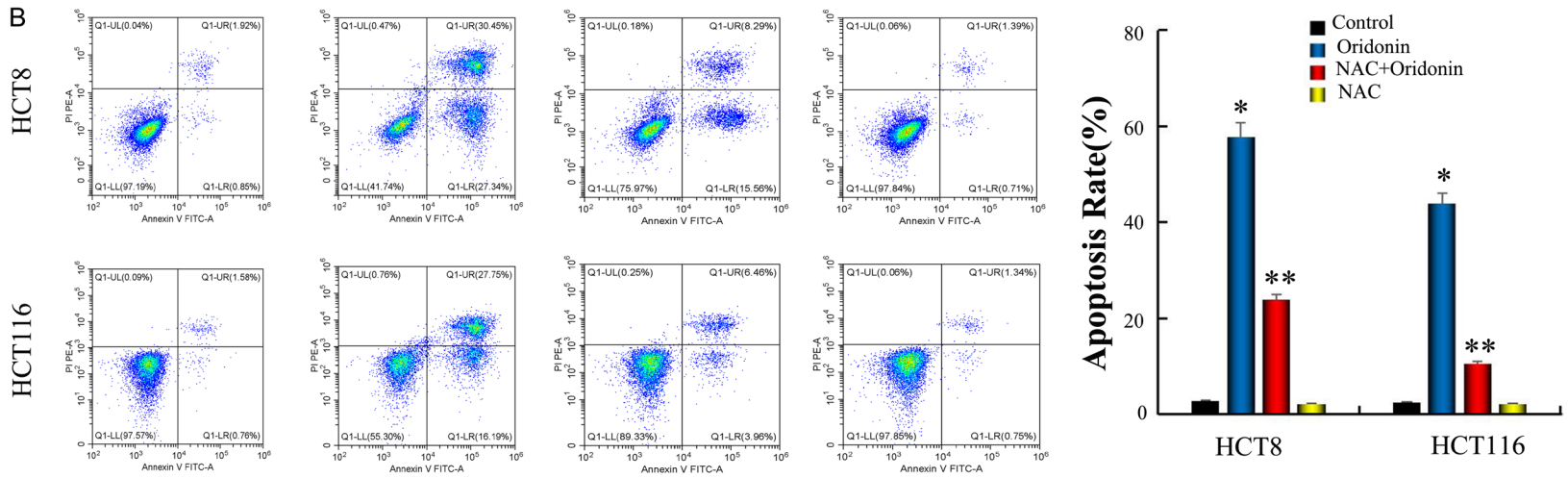

Figure 4. ROS participated in oridonin-induced apoptosis in colon cancer. HCT116 and HCT8 cells were exposed to various concentrations of oridonin (0, 10, 15 and 20 μM) and/or NAC (5 mmol/L) for indicated times. A. The ROS levels were detected by flow cytometry. B. Apoptotic cells were detected by flow cytometry with Annexin V-FITC/PI staining. **P*<0.05 vs control group, ***P*<0.05 vs oridonin (20 μM) group.

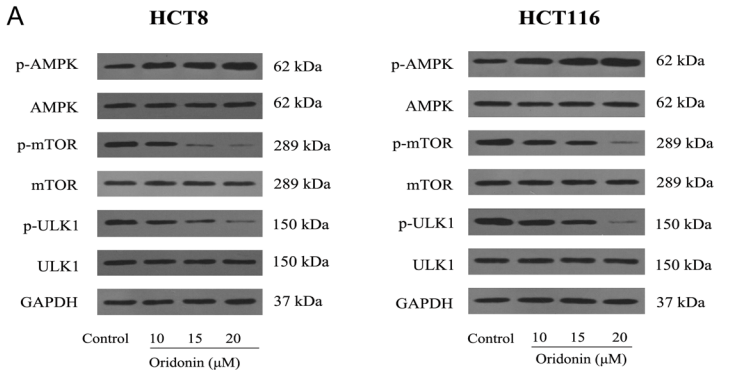
A
HCT8
HCT116
p-AMPK
AMPK
p-mTOR
mTOR
p-ULK1
ULK1
GAPDH
62 kDa
62 kDa
289 kDa
289 kDa
150 kDa
150 kDa
37 kDa
Control 10 15 20
Oridonin (μM)

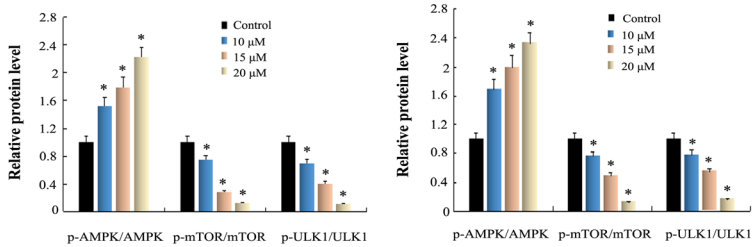
Relative protein level
Control
10 μM
15 μM
20 μM
p-AMPK/AMPK
p-mTOR/mTOR
p-ULK1/ULK1

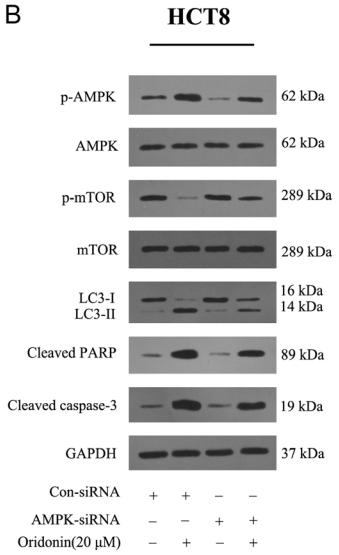
B
HCT8
p-AMPK
AMPK
p-mTOR
mTOR
LC3-I
LC3-II
Cleaved PARP
Cleaved caspase-3
GAPDH
62 kDa
62 kDa
289 kDa
289 kDa
16 kDa
14 kDa
89 kDa
19 kDa
37 kDa
Con-siRNA + + – –
AMPK-siRNA – – + +
Oridonin(20 μM) – + – +

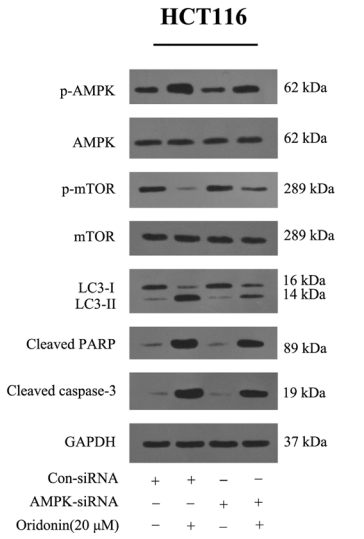
HCT116
p-AMPK
AMPK
p-mTOR
mTOR
LC3-I
LC3-II
Cleaved PARP
Cleaved caspase-3
GAPDH
62 kDa
62 kDa
289 kDa
289 kDa
16 kDa
14 kDa
89 kDa
19 kDa
37 kDa
Con-siRNA + + – –
AMPK-siRNA – – + +
Oridonin(20 μM) – + – +

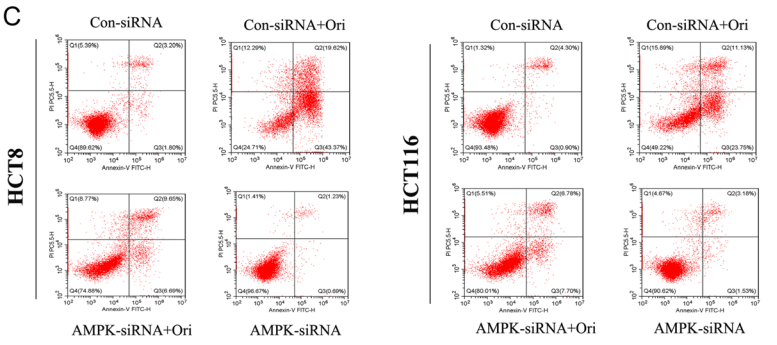
C
HCT8
HCT116
Con-siRNA
Con-siRNA+Ori
AMPK-siRNA+Ori
AMPK-siRNA

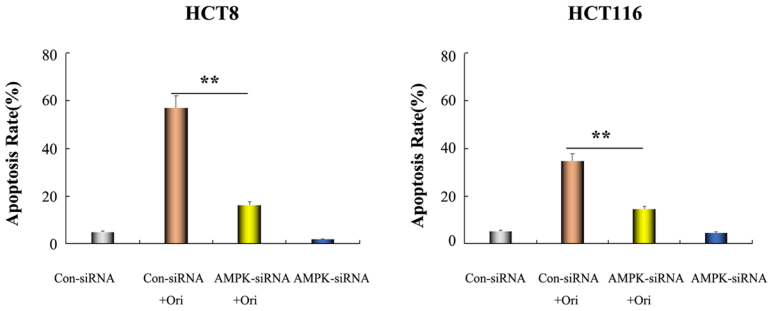
HCT8
HCT116
Apoptosis Rate(%)
**
Con-siRNA
Con-siRNA +Ori
AMPK-siRNA +Ori
AMPK-siRNA

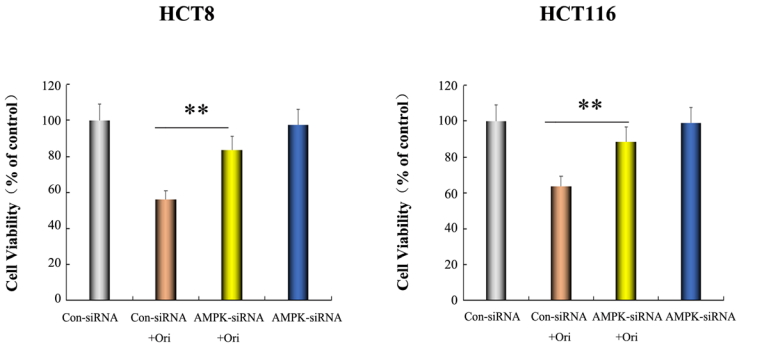
D
HCT8
HCT116
Cell Viability（% of control）
**
Con-siRNA
Con-siRNA +Ori
AMPK-siRNA +Ori
AMPK-siRNA

Figure 5. AMPK-mTOR-ULK1 signaling pathway was involved in oridonin-induced apoptosis in colon cancer. A. HCT116 and HCT8 cells were exposed to various concentratios of oridonin (0, 10, 15 and 20 μM) for 48 h, protein expression levels were detected by western blot analysis. B. Cells were transfected with AMPK-specific siRNA and scrambled siRNA, then incubated with or without 20 μM oridonin for 48 h, and protein expression levels were detected by western blot analysis; C, D. Cell apoptosis and viability were detected by flow cytometry and CCK-8 assay, respectively. *P<0.05 vs Con; **P<0.05 vs Con-siRNA+Ori. Control: Con; Oridonin: Ori.

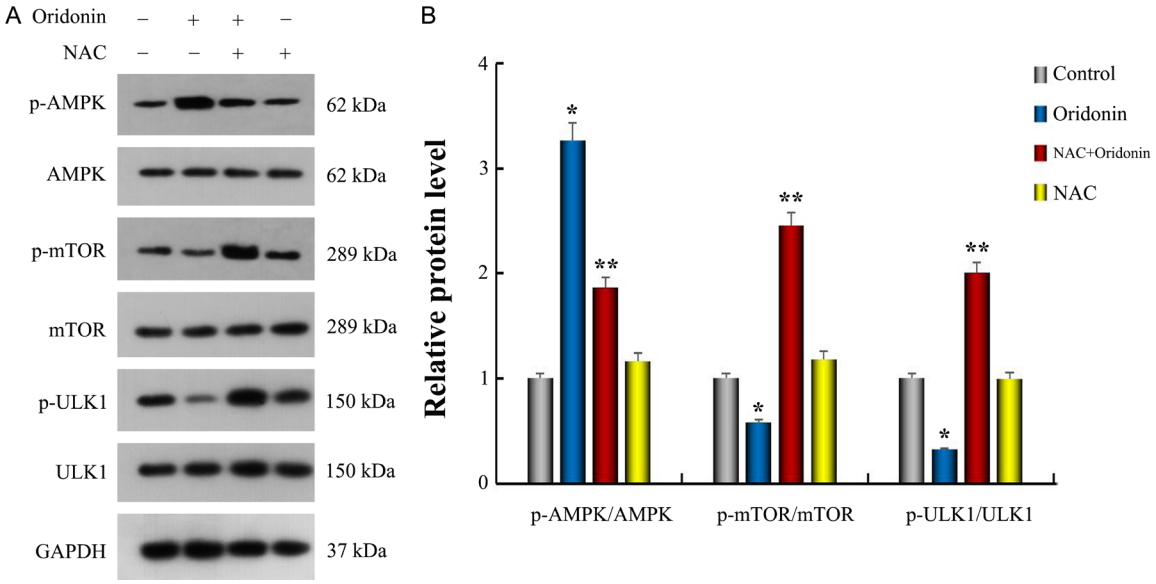

Figure 6. Oridonin-triggered ROS was associated with activation of AMPK-mTOR-ULK1 axis in colon cancer. HCT8 cells were exposed to oridonin (20 μM) with the absence or presence of NAC (5 mmol/L) for 48 h, and protein expression levels were detected by western blot analysis. *P<0.05 vs control group, **P<0.05 vs oridonin (20 μM) group.

lished using HCT8 cells. Compared to the control group, oridonin treatment (5 mg/kg and 10 mg/kg) significantly suppressed tumor growth, with tumor inhibition rates of 39.2% and 66.7%, respectively, without significantly affecting body weight (**Figure 7**). In addition, western blot analysis confirmed increased expression of autophagic (LC3-II) and apoptotic (cleaved caspase-3) markers in tumor tissues following oridonin treatment.

Discussion

Colorectal cancer incidence has been continuously rising globally and remains a major contributor to cancer-related mortality despite advances in treatment. Among the four major modes of cell death (necrosis, apoptosis, autophagy, pyroptosis), apoptosis and autophagy play pivotal roles in tumorigenesis, metastatic progression, and cellular homeostasis. In this study, the effects of oridonin on cell proliferation, cell cycle distribution, autophagy, and apoptosis in colon cancer cells, along with the underlying molecular mechanisms, were investigated. Our results demonstrated that oridonin inhibited proliferation, induced G2/M cell cycle arrest, and triggered both autophagy and apoptosis in colon cancer HCT116 and HCT8 cells. These effects were mediated by the regulation of the ROS-dependent AMPK-mTOR-ULK1 signaling axis.

Oridonin, a bioactive diterpenoid compound, exhibits broad pharmacological activities such as inhibition of proliferation, cell cycle arrest, induction of apoptosis and autophagy. Its anticancer activity is largely attributed to its unique molecular structure, particularly its key pharmacophore, which is the α-methylene cyclopentanone (enone) moiety on the D-ring. Due to its high efficacy, low toxicity, and ability to synergize with chemotherapeutic agents while minimizing adverse effects, oridonin has been widely used in Chinese clinical practice to treat various malignancies [16].

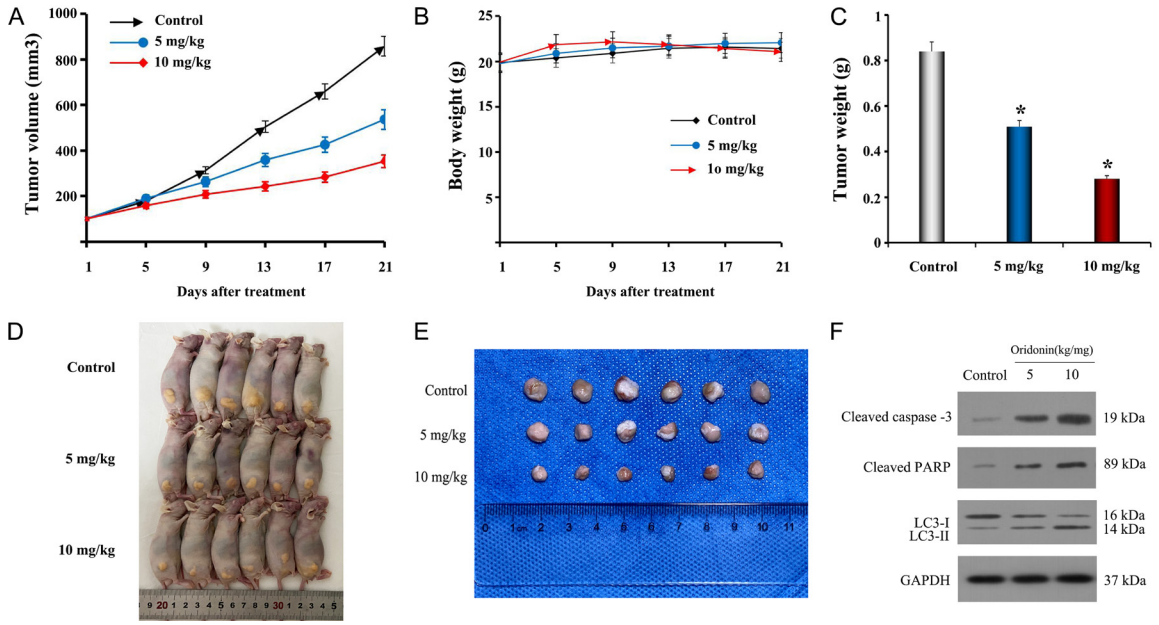

Figure 7. Oridonin suppressed tumor growth in xenograft models. A-E. Tumor volumes, tumor weight and body weight in oridonin (5 or 10 mg/kg)-treated tumor-bearing nude mice. F. The expression of cleaved caspase-3 and LC3-I/II were examined by western blot analysis. *P<0.05 vs control group.

Cancer cells can proliferate indefinitely, becoming essentially immortal under suitable conditions. This uncontrolled growth not only disrupts surrounding tissues and organs but also elicits immune responses, causing further damage. In our study, Oridonin inhibited the proliferation of HCT116 and HCT8 cells in a dose- and time-dependent manner, as confirmed by CCK-8, colony formation, and EdU incorporation assays.

Cell cycle dysregulation is a hallmark of tumorigenesis. The cell cycle comprises four stages, with two major checkpoints at the G1/S and G2/M phases. When abnormalities occur, these checkpoints halt the cycle, allowing DNA repair. If damage persists, the cell undergoes senescence or apoptosis. Flow cytometry analysis in our study showed that oridonin induced G2/M phase arrest, suggesting that it prevents mitosis, thereby contributing to growth inhibition in colon cancer cells.

Cell cycle arrest is often accompanied by apoptosis, a fundamental process in tumor suppression and therapy response [21]. Caspase-3, a key executioner protease, is activated from its inactive form to initiate apoptotic cascades [22]. Flow cytometry and western blot analysis demonstrated that oridonin triggered apoptosis in HCT8 and HCT116 cells, evidenced by increased levels of cleaved caspase-3 and PARP, suggesting caspase-dependent apoptosis. These findings were consistent with previous studies showing that oridonin induces apoptosis in colon cancer cells through different signaling pathways [17-19]. In addition, inhibition of autophagy with 3-MA significantly attenuated oridonin-induced apoptosis, indicating that autophagy is involved in the apoptosis process.

As a critical regulator of cellular homeostasis, autophagy plays context-dependent roles in tumor biology, demonstrating both tumor-suppressive and tumor-promoting capacities. Numerous chemotherapeutic agents have been shown to activate autophagy, which can either promote cell survival or lead to cell death, depending on the cellular context [23]. Autophagy is tightly regulated by autophagy-related genes, with ATG7, LC3, Beclin-1, and p62 as major markers of autophagic activity [24]. ATG7 is crucial for autophagy initiation and autophagosome formation. The development of autophagosomes involves the lipidation of LC3-I to LC3-II, a hallmark of autophagy. Beclin-1, as a core component of the autophagy initiation complex, regulates autophagosome formation and autophagic flux. During

autophagic flux, p62 disrupts the inhibitory interaction between Bcl-2 and Beclin-1, binds to LC3-I/II, and exhibits an inverse relationship with autophagic activity [25]. Evidence also suggests that p62 participates in apoptosis through autophagy-dependent mechanisms, as deletion of its ZZ domain restores sensitivity to apoptotic stimuli [26]. Studies have demonstrated that inducing autophagy can trigger colon cancer cell death [27]. In our study, MDC staining and western blot analysis confirmed that oridonin activated autophagy in HCT8 and HCT116 cells, with reduced p62 and LC3-I levels and increased Beclin-1 and LC3-II expression. Co-treatment with 3-MA reversed these effects by downregulating Beclin-1 and LC3-II, while increasing LC3-I and p62 levels. Apoptosis markers (cleaved caspase-3 and PARP) were also reduced. These findings suggest that autophagy may facilitate oridonin-induced apoptosis in colon cancer cells.

Autophagy and apoptosis play critical roles in determining the fate of neoplastic cells, with their interaction that influences tumor development and resistance mechanisms [28]. In colorectal cancer, their functional interactions can be categorized into three primary modalities based on regulatory mechanisms: (a) autophagy and apoptosis both induce cell death synchronously, or one plays a leading role in promoting cell death (synergistic or collaborative effects); (b) autophagy promotes cell death by inducing apoptosis (promoting effect); and (c) autophagy inhibits apoptosis-induced cell death (antagonistic or inhibitory effect) [29]. Notably, the final classification plays a crucial role in the emergence of cellular drug resistance, contributing to the development of therapy-resistant neoplasms, which pose significant clinical challenges and result in poor survival outcomes [30]. The efficacy of chemotherapy-induced autophagic cell death in malignancies is influenced by multiple factors, including tumor staging, histological origin, and the intensity and persistence of autophagic flux [31]. In tumors, the interplay between autophagy and apoptosis can either act synergistically or antagonistically, depending on the initiating stimulus, which is known as the stressor. Under conditions of nutrient starvation, cellular stress responses typically lead to autophagic cell death as the predominant pathway [32]. The autophagic clearance of damaged organelles facilitates cellular repair and adaptive responses, sustaining viability and homeostasis, whereas defective clearance results in delayed apoptotic activation. In contrast, genotoxic stress or death receptor engagement preferentially triggers rapid apoptotic cascades, with concurrent autophagy supporting the process [33]. Studies have also shown that autophagy and apoptosis are interrelated processes, where suppression of one does not prevent the other, as their respective signaling cascades can activate compensatory mechanisms [34]. If autophagy plays a driving role and precedes apoptosis, it establishes a catabolic state that sustains elevated ATP production, thereby facilitating accelerated apoptotic execution through bioenergetic support [33].

However, the effects of autophagy on tumors and its relationship with apoptosis mainly depend on the intracellular environment, tumor type and tumor development stage. Studies have observed that apoptosis and autophagy occur simultaneously in colorectal cancer cells and tumor-bearing nude mice exposed to chemotherapy or gene interference, causing cell death through their respective regulatory pathways [35-37]. They can also serve as substitutes for each other to cause cell death. For example, autophagy can act as an alternative cell death mechanism in apoptosis-deficient colon cancer HCT116 cells, or promote cell death in apoptosis-resistant SW620 Ad300 cells. Similarly, apoptosis can induce cell death in autophagy-deficient colon cancer HCT116 cells [38-40]. Autophagy inhibitors or silencing of autophagy genes can inhibit apoptosis, suggesting that autophagy may promote apoptosis. For example, the natural compound trifolirhizin induces autophagy-associated apoptosis in colon malignancies by modulating the AMPK-mTOR signaling axis [41]. In addition, autophagy inhibitors or gene silencing can promote apoptosis. For example, artesunate and myricetin induce both autophagy and apoptosis in colon cancer cells, and inhibition of autophagy can enhance the induced apoptosis, suggesting that autophagy may protect cells by inhibiting apoptosis [42, 43]. Studies have shown that inhibition of autophagy in colon cancer cells treated with the pan-caspase inhibitor Z-VAD-FMK leads to a reduction in autophagic activity, indicating that apoptosis may act as an upstream activator of autophagy in cells of

colon cancer [44]. Our experimental data demonstrated that oridonin treatment simultaneously triggered apoptotic and autophagic responses in HCT8 and HCT116 cells, although the relationship between the two processes was unclear. Further investigation of the effects of oridonin combined with the autophagy inhibitor 3-MA on cell proliferation, apoptosis, and autophagy revealed that 3-MA reduced the number of autophagic cell deaths. MDC-based autophagic vesicle detection showed a significant reduction in autophagosomes in the presence of 3-MA, while western blotting revealed reversible changes in autophagy-related proteins (p62, Beclin1, LC3-I/II) after co-treatment with oridonin and 3-MA, highlighting the role of autophagy in oridonin-induced antiproliferation. In addition, flow cytometry and western blot analysis demonstrated that co-treatment with 3-MA reversed the apoptotic effects of oridonin in HCT8 and HCT116 cells. These findings suggest that inhibition of autophagy could reduce oridonin-induced apoptosis. To explore the role of autophagy in oridonin-induced apoptosis, MDC staining revealed increased autophagosomes after the addition of the apoptosis inhibitor Z-VAD-FMK. Western blot analysis showed that co-treatment with Z-VAD-FMK attenuated the proteolytic activation of caspase-3 and PARP but promoted LC3-II expression, suggesting that suppression of apoptosis increases autophagic activity and that autophagy may compensate for apoptotic cell death. These findings indicate that oridonin's antiproliferative effects arise from its dual induction of apoptotic and autophagic pathways. Autophagy may enhance cell death through synergistic interactions with apoptosis.

Substantial evidence supports the idea that supraphysiological ROS levels trigger cytotoxic effects in malignant cells, culminating in oncotic cell death [18, 45, 46]. Our experimental data demonstrated a significant ROS accumulation in HCT116 and HCT8 cells treated with oridonin. Notably, NAC-mediated ROS scavenging significantly reduced apoptotic rates, suggesting that ROS are a key mediator of oridonin's antitumor effects.

Autophagy is regulated by several signaling networks, with the AMPK-mTOR-ULK1 pathway being particularly influential [47]. mTOR, a serine/threonine kinase, regulates cellular growth and proliferation. Under nutrient deprivation, mTORC1 is inhibited, stimulating autophagy. Conversely, mTOR activation inhibits autophagy by phosphorylating ULK1 at Ser757 [48]. AMPK, a key regulator of cell energy homeostasis, acts as a tumor suppressor by regulating inflammatory responses, programmed cell death, and autophagic flux [49]. AMPK activation relieves mTOR-dependent inhibition at ULK1 Ser757, promoting autophagy [50-52]. Our western blot analysis showed that oridonin induced AMPK activation, leading to reduced p-mTOR and p-ULK1 levels, thereby triggering autophagy in colon cancer cells. This finding was also consistent with previous studies showing that AMPK can promote cell death by inhibiting mTORC1 and activating ULK1 [20, 51]. To further verify the role of AMPK in this pathway, AMPK-specific siRNA was used to silence AMPK. Western blot analysis revealed that AMPK silencing abolished oridonin's effects, reversing the activation of p-AMPK and inhibition of p-mTOR AMPK. Moreover, the effects of oridonin on autophagy-related proteins (LC3-I/II) and pro-apoptotic proteins (cleaved caspase-3/PARP) were reversed after AMPK silencing. CCK-8 assays and flow cytometry confirmed that AMPK silencing partially attenuated oridonin's antiproliferative and pro-apoptotic effects in colon cancer cells, suggesting that activated AMPK negatively regulates the mTOR pathway, influencing downstream apoptosis- and autophagy-related proteins and inhibiting cell growth. These data indicate that the AMPK-mTOR cascade plays an important role in the initiation of autophagy and apoptosis, contributing to the growth inhibition induced by oridonin.

The AMPK-mTOR-ULK1 signaling pathway, the main pathway regulating autophagy, can be activated by ROS [11-13]. Previous studies have reported that oridonin could increase ROS levels in colon cancer cells [14, 15], which was also confirmed in our study using HCT116 and HCT8 cells. In addition, the ROS scavenger NAC effectively suppressed both oridonin-induced ROS generation and activation of the AMPK-mTOR-ULK1 pathway, consequently reducing apoptosis. These results suggest that ROS generation is a prerequisite for the activation of the AMPK-Mtor-ULK1 pathway, acting as the critical mediator of oridonin's antitumor activity in colon cancer.

Finally, *in vivo* studies demonstrated that oridonin dose-dependently inhibited the growth of

HCT8 xenograft tumors in nude mice without significant loss of body weight. Western blot analysis of tumor tissues showed increased expression of LC3-II and cleaved caspase-3 following oridonin treatment, indicating that oridonin also induces autophagy and apoptosis *in vivo*, thereby contributing to colon cancer suppression.

Conclusion

In summary, oridonin induced ROS-mediated activation of AMPK, which inhibited the mTOR-ULK1 axis, thereby inducing both autophagy and apoptosis in colon cancer cells. Autophagy further promoted apoptotic cell death. Collectively, our findings revealed that oridonin exerted antitumor effects through ROS-dependent activation of the AMPK-mTOR-ULK1 axis, ultimately triggering autophagy-dependent apoptosis. These results provide an experimental basis for colon cancer treatment and a theoretical foundation for the anticancer potential of other terpenoids and traditional Chinese medicines targeting autophagy-related signaling pathways.

Acknowledgements

The authors would like to thank the Animal Experimental Research Center in Zhejiang Academy of Traditional Chinese Medicine for technical assistance. This study was supported by Science and Technology project of traditional Chinese medicine in Zhejiang province, China (Grant No. 2023ZL343) and the medical and health research project of Zhejiang Province (Grant No. 2025KY289).

Disclosure of conflict of interest

None.

Address correspondence to: Dr. Heqi Bu, Department of Colorectal Surgery, Beilun District People's Hospital (Beilun Branch of The First Affiliated Hospital of Zhejiang University School of Medicine), 1288 Lu-Shan East Road, Beilun District, Ningbo 315800, Zhejiang, The People's Republic of China. E-mail: buheqi@163.com; blrmyybgs@163.com

References

[1] Wu Y, He S, Cao M, Teng Y, Li Q, Tan N, Wang J, Zuo T, Li T, Zheng Y, Xia C and Chen W. Comparative analysis of cancer statistics in China and the United States in 2024. Chin Med J (Engl) 2024; 137: 3093-3100.

[2] Liu W, Wang Y, Xia L and Li J. Research progress of plant-derived natural products against drug-resistant cancer. Nutrients 2024; 16: 797.

[3] Orlandi G, Roncucci L, Carnevale G and Sena P. Different roles of apoptosis and autophagy in the development of human colorectal cancer. Int J Mol Sci 2023; 24: 10201.

[4] Liu S, Yao S, Yang H, Liu S and Wang Y. Autophagy: regulator of cell death. Cell Death Dis 2023; 14: 648.

[5] Zhang J, Xiang Q, Wu M, Lao YZ, Xian YF, Xu HX and Lin ZX. Autophagy regulators in cancer. Int J Mol Sci 2023; 24: 10944.

[6] Cheung EC and Vousden KH. The role of ROS in tumour development and progression. Nat Rev Cancer 2022; 22: 280-297.

[7] Chok KC, Koh RY, Ng MG, Ng PY and Chye SM. Melatonin induces autophagy via reactive oxygen species-mediated endoplasmic reticulum stress pathway in colorectal cancer cells. Molecules 2021; 26: 5038.

[8] Lu Q, Xu S, Hao Z, Li Y, Huang Y, Ying S, Jing W, Zou S, Xu Y and Wang H. Dinotefuran exposure induces autophagy and apoptosis through oxidative stress in Bombyx mori. J Hazard Mater 2023; 458: 131997.

[9] Hsu CC, Peng D, Cai Z and Lin HK. AMPK signaling and its targeting in cancer progression and treatment. Semin Cancer Biol 2022; 85: 52-68.

[10] Fu W and Wu G. Targeting mTOR for anti-aging and anti-cancer therapy. Molecules 2023; 28: 3157.

[11] Lu H, Mei C, Yang L, Zheng J, Tong J, Duan F, Liang H and Hong L. PPM-18, an analog of vitamin K, induces autophagy and apoptosis in bladder cancer cells through ROS and AMPK signaling pathways. Front Pharmacol 2021; 12: 684915.

[12] Zhou X, Chen Y, Wang F, Wu H, Zhang Y, Liu J, Cai Y, Huang S, He N, Hu Z and Jin X. Artesunate induces autophagy dependent apoptosis through upregulating ROS and activating AMPK-mTOR-ULK1 axis in human bladder cancer cells. Chem Biol Interact 2020; 331: 109273.

[13] Song CF, Hu YH, Mang ZG, Ye Z, Chen HD, Jing DS, Fan GX, Ji SR, Yu XJ, Xu XW and Qin Y. Hernandezine induces autophagic cell death in human pancreatic cancer cells via activation of the ROS/AMPK signaling pathway. Acta Pharmacol Sin 2023; 44: 865-876.

[14] Sun J, Feng Y, Wang Y, Ji Q, Cai G, Shi L, Wang Y, Huang Y, Zhang J and Li Q. α-hederin induces autophagic cell death in colorectal cancer cells through reactive oxygen species depen-

dent AMPK/mTOR signaling pathway activation. Int J Oncol 2019; 54: 1601-1612.
[15] Wang GY, Zhang L, Geng YD, Wang B, Feng XJ, Chen ZL, Wei W and Jiang L. β-Elemene induces apoptosis and autophagy in colorectal cancer cells through regulating the ROS/AMPK/mTOR pathway. Chin J Nat Med 2022; 20: 9-21.
[16] Li X, Zhang CT, Ma W, Xie X and Huang Q. Oridonin: a review of its pharmacology, pharmacokinetics and toxicity. Front Pharmacol 2021; 12: 645824.
[17] Chen F, Liao J, Wu P, Cheng L, Ma Y, Zhang L, Leng X, Zhu X, Liu Z and Xie F. Oridonin inhibits the occurrence and development of colorectal cancer by reversing the Warburg effect via reducing PKM2 dimer formation and preventing its entry into the nucleus. Eur J Pharmacol 2023; 954: 175856.
[18] Zhang D, Zhou Q, Huang D, He L, Zhang H, Hu B, Peng H and Ren D. ROS/JNK/c-Jun axis is involved in oridonin-induced caspase-dependent apoptosis in human colorectal cancer cells. Biochem Biophys Res Commun 2019; 513: 594-601.
[19] Bu HQ, Shen F and Cui J. The inhibitory effect of oridonin on colon cancer was mediated by deactivation of TGF-β1/Smads-PAI-1 signaling pathway in vitro and vivo. Onco Targets Ther 2019; 12: 7467-7476.
[20] Bu H, Liu D, Zhang G, Chen L and Song Z. AMPK/mTOR/ULK1 axis-mediated pathway participates in apoptosis and autophagy induction by oridonin in colon cancer DLD-1 cells. Onco Targets Ther 2020; 13: 8533-8545.
[21] Chaudhry GE, Akim AM, Sung YY and Muhammad TST. Cancer and apoptosis. Methods Mol Biol 2022; 2543: 191-210.
[22] Eskandari E and Eaves CJ. Paradoxical roles of caspase-3 in regulating cell survival, proliferation, and tumorigenesis. J Cell Biol 2022; 221: e202201159.
[23] Cheng X, Feng H, Wu H, Jin Z, Shen X, Kuang J, Huo Z, Chen X, Gao H, Ye F, Ji X, Jing X, Zhang Y, Zhang T, Qiu W and Zhao R. Targeting autophagy enhances apatinib-induced apoptosis via endoplasmic reticulum stress for human colorectal cancer. Cancer Lett 2018; 431: 105-114.
[24] Zhang J, Xiang Q, Wu M, Lao YZ, Xian YF, Xu HX and Lin ZX. Autophagy regulators in cancer. Int J Mol Sci 2023; 24: 10944.
[25] Devis-Jauregui L, Eritja N, Davis ML, Matias-Guiu X and Llobet-Navàs D. Autophagy in the physiological endometrium and cancer. Autophagy 2021; 17: 1077-1095.
[26] Islam MA, Sooro MA and Zhang P. Autophagic regulation of p62 is critical for cancer therapy. Int J Mol Sci 2018; 19: 1405.
[27] Song C, Xu W, Wu H, Wang X, Gong Q, Liu C, Liu J and Zhou L. Photodynamic therapy induces autophagy-mediated cell death in human colorectal cancer cells via activation of the ROS/JNK signaling pathway. Cell Death Dis 2020; 11: 938.
[28] Booth LA, Roberts JL and Dent P. The role of cell signaling in the crosstalk between autophagy and apoptosis in the regulation of tumor cell survival in response to sorafenib and neratinib. Semin Cancer Biol 2020; 66: 129-139.
[29] Xie Q, Liu Y and Li X. The interaction mechanism between autophagy and apoptosis in colon cancer. Transl Oncol 2020; 13: 100871.
[30] Liu T, Zhang J, Li K, Deng L and Wang H. Combination of an autophagy inducer and an autophagy inhibitor: a smarter strategy emerging in cancer therapy. Front Pharmacol 2020; 11: 408.
[31] Jin C, Wang T, Yang Y, Zhou P, Li J, Wu W, Lv X, Ma G and Wang A. Rational targeting of autophagy in colorectal cancer therapy: from molecular interactions to pharmacological compounds. Environ Res 2023; 227: 115721.
[32] Gundamaraju R, Lu W, Paul MK, Jha NK, Gupta PK, Ojha S, Chattopadhyay I, Rao PV and Ghavami S. Autophagy and EMT in cancer and metastasis: who controls whom? Biochim Biophys Acta Mol Basis Dis 2022; 1868: 166431.
[33] Sorice M. Crosstalk of autophagy and apoptosis. Cells 2022; 11: 1479.
[34] Das S, Shukla N, Singh SS, Kushwaha S and Shrivastava R. Mechanism of interaction between autophagy and apoptosis in cancer. Apoptosis 2021; 26: 512-533.
[35] Li S, Wang X, Wang G, Shi P, Lin S, Xu D, Chen B, Liu A, Huang L, Lin X and Yao H. Ethyl acetate extract of selaginella doederleinii hieron induces cell autophagic death and apoptosis in colorectal cancer via PI3K-Akt-mTOR and AMPKα-signaling pathways. Front Pharmacol 2020; 11: 565090.
[36] Zhang Y, Liu Y, Zhou Y, Zheng Z, Tang W, Song M, Wang J and Wang K. Lentinan inhibited colon cancer growth by inducing endoplasmic reticulum stress-mediated autophagic cell death and apoptosis. Carbohydr Polym 2021; 267: 118154.
[37] Woźniak M, Makuch S, Winograd K, Wiśniewski J, Ziółkowski P and Agrawal S. 6-Shogaol enhances the anticancer effect of 5-fluorouracil, oxaliplatin, and irinotecan via increase of apoptosis and autophagy in colon cancer cells in hypoxic/aglycemic conditions. BMC Complement Med Ther 2020; 20: 141.
[38] Xiong HY, Guo XL, Bu XX, Zhang SS, Ma NN, Song JR, Hu F, Tao SF, Sun K, Li R, Wu MC and Wei L. Autophagic cell death induced by 5-FU

in Bax or PUMA deficient human colon cancer cell. Cancer Lett 2010; 288: 68-74.
[39] Hu T, Wang L, Zhang L, Lu L, Shen J, Chan RL, Li M, Wu WK, To KK and Cho CH. Sensitivity of apoptosis-resistant colon cancer cells to tanshinones is mediated by autophagic cell death and p53-independent cytotoxicity. Phytomedicine 2015; 22: 536-44.
[40] Amin A, Bajbouj K, Koch A, Gandesiri M and Schneider-Stock R. Defective autophagosome formation in p53-null colorectal cancer reinforces crocin-induced apoptosis. Int J Mol Sci 2015; 16: 1544-61.
[41] Sun D, Tao W, Zhang F, Shen W, Tan J, Li L, Meng Q, Chen Y, Yang Y and Cheng H. Trifolirhizin induces autophagy-dependent apoptosis in colon cancer via AMPK/mTOR signaling. Signal Transduct Target Ther 2020; 5: 174.
[42] Jiang F, Zhou JY, Zhang D, Liu MH and Chen YG. Artesunate induces apoptosis and autophagy in HCT116 colon cancer cells, and autophagy inhibition enhances the artesunate-induced apoptosis. Int J Mol Med 2018; 42: 1295-1304.
[43] Zhu ML, Zhang PM, Jiang M, Yu SW and Wang L. Myricetin induces apoptosis and autophagy by inhibiting PI3K/Akt/mTOR signalling in human colon cancer cells. BMC Complement Med Ther 2020; 20: 209.
[44] Wang L, Hu T, Shen J, Zhang L, Chan RL, Lu L, Li M, Cho CH and Wu WK. Dihydrotanshinone I induced apoptosis and autophagy through caspase dependent pathway in colon cancer. Phytomedicine 2015; 22: 1079-87.
[45] Kohan R, Collin A, Guizzardi S, Tolosa de Talamoni N and Picotto G. Reactive oxygen species in cancer: a paradox between pro- and anti-tumour activities. Cancer Chemother Pharmacol 2020; 86: 1-13.
[46] Hu X, Huang S, Ye S and Jiang J. The natural product oridonin as an anticancer agent: current achievements and problems. Curr Pharm Biotechnol 2024; 25: 655-664.
[47] Zhang Y, He N, Zhou X, Wang F, Cai H, Huang SH, Chen X, Hu Z and Jin X. Betulinic acid induces autophagy-dependent apoptosis via Bmi-1/ROS/AMPK-mTOR-ULK1 axis in human bladder cancer cells. Aging (Albany NY) 2021; 13: 21251-21267.
[48] Fu W and Wu G. Targeting mTOR for anti-aging and anti-cancer therapy. Molecules 2023; 28: 3157.
[49] Hsu CC, Peng D, Cai Z and Lin HK. AMPK signaling and its targeting in cancer progression and treatment. Semin Cancer Biol 2022; 85: 52-68.
[50] Lin M, Hua R, Ma J, Zhou Y, Li P, Xu X, Yu Z and Quan S. Bisphenol A promotes autophagy in ovarian granulosa cells by inducing AMPK/mTOR/ULK1 signalling pathway. Environ Int 2021; 147: 106298.
[51] Xiang X, Tian Y, Hu J, Xiong R, Bautista M, Deng L, Yue Q, Li Y, Kuang W, Li J, Liu K, Yu C and Feng G. Fangchinoline exerts anticancer effects on colorectal cancer by inducing autophagy via regulation AMPK/mTOR/ULK1 pathway. Biochem Pharmacol 2021; 186: 114475.
[52] Park JM, Lee DH and Kim DH. Redefining the role of AMPK in autophagy and the energy stress response. Nat Commun 2023; 14: 2994.